www.ThePharmaJournal.com

The Pharma Innovation

ISSN (E): 2277- 7695
ISSN (P): 2349-8242
NAAS Rating: 5.23
TPI 2021; SP-10 (5): 91-105

www.thepharmajournal.com
Received: 06-03-2021
Accepted: 15-04-2021

K Nagaraju
PhD Scholar, Department of Soil Science and Agricultural Chemistry, SV Agricultural College, ANGRAU, Tirupati, Andhra Pradesh, India

TNVKV Prasad
Principal Scientist, Department of Soil Physics, Nanotechnology Laboratory, IFT, RARS, Tirupati, Andhra Pradesh, India

V Munaswamy
Professor, Department of Soil Science and Agricultural Chemistry, SV Agricultural College, ANGRAU, Tirupati, Andhra Pradesh, India

Y ReddiRamu
Associate Professor, Department of Agronomy, SV Agricultural College, ANGRAU, Tirupati, Andhra Pradesh, India

Corresponding Author:
K Nagaraju
PhD Scholar, Department of Soil Science and Agricultural Chemistry, SV Agricultural College, ANGRAU, Tirupati, Andhra Pradesh, India

A novel approach for the extraction of nanoclay particles from vertisols and alfisols and their spectral characterization

K Nagaraju, TNVKV Prasad, V Munaswamy and Y ReddiRamu

Abstract
The present study emphasized on the differences in the spectrochemical and optical characteristics of clay particles extracted from various regions of Andhra Pradesh which were categorized into black and red soils. From the DLS analysis, no significant differences were noticed in the size of the particles (ranged from 9.8 to 47.8 nm) as well as in their viscosity (range from 0.892-0.895) in both types. However, we have observed a wide range of difference in the zeta potential. The nanoclay particles extracted from black soil were observed to be less stable with a least zeta potential of + 22.5 mV and red soil with high stability and dispersion with a highest zeta potential of -69 mV. FTIR data revealed presence of carboxylic acid salts (1523 cm-1), phosphate (900 cm-1) and silicon ions (1100 cm-1), thiols/ethers (684 cm-1) were commonly present in all the samples irrespective of black and red soils but alkyl carbonates (1742 cm-1) were seen in all black soil samples and also exclusively in the red soil. The crystal structure analyses revealed that Kaolin was present exclusively in the clay samples of coastal regions (7 Å spacing) and rectorite characteristic to 25.0 Å spacing was seen in both types of soil and also Montmorilonites (17.7 Å) was detected in some samples. Electron microscopic images showed curved and matted flakes and a combination of spiny and flocculating flakes shaped nanoclay particles extracted from black soils. Curved and matted flakes and a combination of spiny and flocculating flakes shaped nanoclay particles have been observed which were extracted from the red soils.

Keywords: Black soils, red soils, clay particles, montmorillonite, flocculating flakes

Introduction
Nanotechnology is an emerging field in the area of interdisciplinary research, especially in biology. The advancement of nanotechnology mainly requires the development of reliable and eco-friendly protocols for the synthesis of nanomaterial over a range of biological composition, sizes, shapes and high monodispersity. Nanotechnology is concerned with the design, synthesis and use of materials at the nanoscale level, ranging from 1 to 100 nm. The term ‘nano’ comes from the Greek nano, meaning dwarf and when used as a prefix indicates 10-9 m. Nanoparticles possess exceptional physical and chemical properties which lead to rapid commercialization. Nanoparticles are considered as fundamental molecular building blocks for nanotechnology. They are the pre-requisites for preparing many nanostructure materials and devices. In nanoscience, material design and surface feature of nanomaterials play an increasing role in many fields of technological application such as electronics, medicine, bio-catalysis, materials science and others. Although synthetic nanomaterials are relevant for a wide possibility of applications in nanoscience (Garrido *et al*., 2010) [9], the production of nanoparticle with small diameters and a narrow size distribution is expensive and difficult (Hofmann *et al*., 2008) [11].
NPs occur widely in the natural environment (Theng and Yuan., 2008) [28]. Particles within nanoscale range were studied in soil sciences a few decades ago to understand the behavior of soil environment (Wada 1987; Parffit *et al*., 1983) [30, 31]. In the environment we can find many types of morphologies that actually are synthesized, thereby an interesting alternative is to obtain and use natural nanomaterials. Nanoparticles (NPs) have broad applications in science and engineering (Diallo and Savage, 2005; Aitken *et al*., 2006; Tratnyek and Johnson, 2006) [2, 7]. Natural nanoparticles usually exist in soils, sediments, volcanic dust, ash, ice cores, ocean surface microlayers, freshwater and other natural waters and are composed of clay minerals, metal hydroxy oxides, carbonates and humic substances (Murr *et al*., 2004; Waychunas *et al*., 2005; Floody *et al*., 2009) [8, 21, 32].

Research on the bio-geochemical and ecological effects of natural NPs is growing fast (Hochella *et al*., 2008) [10]. NPs vary in size, ranging from a few to several tens of nm and have complex chemical properties. It has been established that the particle size of NPs is important in biogeochemical reactions and kinetics (Hochella *et al*., 2008) [10]. Natural NPs have large sorption capacities for metals and anionic contaminants such as chromium, lead, mercury, selenium and arsenic (Waychunas *et al*., 2005; Hochella *et al*., 2008) [10, 32], good capacities in enhancing contaminant transport (Ryan and Elimelech, 1996) [26] and play an important role in geo catalysis because of their large surface area (Wilson *et al*., 2008) [33]. Therefore, natural NPs could strongly influence the solubility, transport, degradation and bioavailability of environmental pollutants (Pranzas *et al*., 2003) [25]. Of all the media in which natural NPs are present, the soil system is especially reactive and complex. Although soil NPs has been isolated with a single composition, such as allophane and iron oxide minerals (Nowack and Bucheli, 2007; Floody *et al*., 2009) [8, 23], most soil-derived NPs have a complex composition affected by soil properties. More comprehensive studies on natural soil NPs are required in order to understand their composition, properties and roles in the bio-geochemical cycle.

Clay minerals (size < 2 µm) are widely distributed in the surface of the earth with the characteristics of small size, and they significantly affect the physical, chemical and biological processes of soils (Cebron *et al*., 2015) [6]. Additionally, clay minerals undergo spontaneous modification and transformation with the change of environmental conditions, which can be illustrated by the structures and types of clay minerals (Turpault *et al*., 2008) [29].

Clays which have size <100 nm in at least one dimension are referred as nanoclays (Floody *et al*., 2009) [8]. Nanoclay is a real alternative to get a natural material with nanometric size. These nanoclays excel non-nano fraction of clays in terms of specific surface area, CEC, surface charge density and surface reactivity. Nanoclays mostly occur in smectite and non-crystalline amorphous aluminosilicate fractions of soils. Nanoclays have been employed as fillers in polymers to improve their mechanical performance, thermal stability, barrier properties and flame retardancy. Various kinds of nanoclays such as montmorillonite, kaolinite, hectorite and saponite have attracted the great attention of scientists and technologists within both academia and industrial area (Lepoittevin *et al*., 2002; Jeon *et al*., 2003) [13, 16]. Clay minerals are hydrous silicates and may simply be described as fine-grained particles with the sheet-like structure stacked over one another, they are commonly known as phyllosilicates, sheet-structured silicates. Phyllosilicates are mainly composed of fine-grained aluminosilicates and are formed as a result of chemical weathering of silicate minerals at the surface of the earth (Majeed *et al*., 2013; Zhang *et al*., 2010) [20, 34].

In soils derived from volcanic ashes such as Andisols (Calabi *et al*., 2009), have different structures of nanoparticles like aluminosilicate with nano-ball (allophane) and nano-tube (imogolite) morphology (Wada 1987; Abidin *et al*., 2007) [30, 31]. The most important constituent of Andisols is allophane which is a non-crystalline aluminosilicate with Al/Si ratio varying between 1 and 2. The Independent composition of the unit particle of allophane is a hollow spherule with an outer diameter of 3.5–5.0 nm. Imogolite is more crystalline than allophane. The unit particle of imogolite is a hollow tubule with an outer and inner diameter of about two and one nm, respectively (Abidin *et al*., 2007) [1].

Nanoclays may be separated from the clay fraction or from the bulk clay material by different approaches. Methods used for extracting and processing of nanoclays including energetic stirring followed by centrifugation and freeze-drying; centrifugation and cross-flow filtration; and ultracentrifugation (Floody *et al*., 2009) [8]. Major research domains include (i) synthesis and characterization: (ii) surface properties and stability; (iii) fabrication of nanoclay-filled nanocomposites; and (iv) the use of nanoclays as precursors for the development of novel materials. Nanoclays have found applications in many fields including medicine, pharmacy, cosmetics, food packing and textile industry.

Materials and Methods

The present study was carried out to extract nanoclay particles in black and red soils, standardization of method of extraction of nanoclays and characterization of nanoclay particles. The Soil samples were collected in different places of Andhra Pradesh.

Details of soil samples collected

Soil samples were collected from ten locations in different districts of Andhra Pradesh namely Kambaladinne, Rekulakunta, Anakapalli, Lamfaram, Rajamahendravaram, Garikapadu, *Vizi*anagaram, Tirupati, Utukur, and Maruteru villages. Soil samples were collected up to a depth of 20 cm. Around 1 kg soil was collected precisely into a transparent polythene bags and labeled properly.

Soil samples were collected from different locations of Andhra Pradesh as detailed below.

Kambaladinne village is located at 15º 47’ North latitude and 77º 20’ East longitude at an altitude of 361 m above mean sea level.

Lam farm, Guntur is located at 16º 21’ North latitude and 80º 26’ East longitude at an altitude of 39 m above mean sea level.

Rajamahendravaram is located at 17º 02’ North latitude and 81º 46’ East longitude at an altitude of 24 m above mean sea level.

Garikapadu village is located at 16º 57’ North latitude and 80º 03’ East longitude at an altitude of 31 m above mean sea level.

Maruteru is located at 16º 37’ North latitude and 81º 44’ East longitude at an altitude of 9 m above mean sea level.

Rekulakunta village is located at 14º 41’ North latitude and 77º 40’ East longitude at an altitude of 347 m above mean sea level.

Anakapalli is located at 17º 42’ North latitude and 83º 00’ East longitude at an altitude of 31 m above mean sea level.

*Vizi*anagaram is located at 18º 07’ North latitude and 83º 23’ East longitude at an altitude of 65 m above mean sea level.

Tirupati is located at 13º 39’ North latitude and 79.16º 26’ East longitude at an altitude of 39 m above mean sea level.

Utukur village is located at 14º 21’ North latitude and 78º 48’ East longitude at an altitude of 138 m above mean sea level.

Location of work

The present work was carried out in the Department of Soil Science and Agricultural Chemistry, S.V. Agricultural College, Tirupati and Nanotechnology Laboratory, Institute of Frontier Technology (IFT), Regional Agricultural Research Station, Tirupati of Acharya N. G. Ranga Agricultural University.

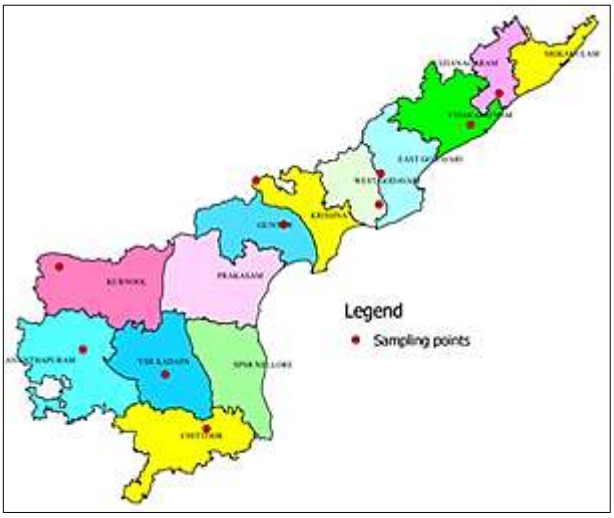

Fig 1: Locations of soil sample in different districts of Andhra Pradesh

Processing of soil samples

The samples were air dried under shade, ground with the wooden mallet, sieved through a 2 mm sieve and preserved in polyethylene bags for further laboratory studies.

Clay mineralogy

Clay separation

Clay in the soil sample collected from different locations was separated by following the procedure outlined by Jackson (1973) [12].

Extraction of nanoclay particles from black and red soils

The nanoclay fraction was extracted using a modified method as described by Li and Hu (2003) [17]. Briefly, 1 g of the clay was suspended in 50 mL of 1 M NaCl, ultrasonicated at 4280 J g^{-1}, (selected from 3000 to 5000 J g^{-1} range tested) for 3 min, the slurry was then centrifuged at 3000 rpm for 40 min. The upper solution was discarded, and the sediment was washed with 50 ml of pure water under moderate stirring. The resulting slurry was centrifuged again, and the upper dispersion was collected. This procedure was repeated 11 times. The collected supernatants, containing the nanoclay, were dialyzed (1000 kDa membrane) against deionized water until the conductivity of the water reached 0.5–0.8 µS cm^{-1}. The dialyzed material was freeze-dried to yield solid nanoclay particles.

Characterization of nanoclay particles UV-VIS spectroscopy

The spectra of the surface Plasma resonance of NPs in the reaction mixture were recorded using UV–VIS spectrophotometer (Shimadzu, UV-2450) at wavelengths between 240 and 280 nm.

Nano particle size distribution

The aqueous suspension of the synthesized nanoparticles was filtered through a 0.22 µm syringe driven filter unit and the size of the nanoparticles was measured by using the principle of Dynamic Light Scattering (DLS) technique made in a (Horiba Scientific Nanopartica SZ-100, Japan) series compact scattering spectrometer (Kuzniatsova *et al.,* 2007) [15]. In the particle size analyzer, particle size was measured by photon correlation method in the range of 0.30 nm to 8.00 µm and a data acquisition time was less than two minutes. The cell holder temperature was controlled from 1 to 90 °C whereas for electrode and plastic cell it was 1 to 70 °C. The laser light went through an ND-filter and the lenses were set at the optical strength when the input to the sample particles in the cell. The particle size measurement was done at 90 or 173 degree angle. During the experiment, 10 mg of sample was taken in a beaker and 50 ml of ultrapure water was added and sonicated for 30 min. in an ultrasonicator. The size of samples was measured using particle size analyzer.

Zeta potential measurements

The aqueous suspension of the synthesized nanoparticles was determined by measuring the zeta potential. The zeta potential of the supernatant aqueous solution was determined using Zeta analyzer (Horiba Scientific Nanopartica SZ-100, Japan). The suspension measured the size distribution of the particle, average diameter and zeta potential (Asadi *et al.,* 2009) [3]. In the zeta analyzer, zeta potential measurement varied from -200 mV to 200 mV as data acquisition time is usually less than one minute for zeta potential measurement. Ten mg of sample was taken in a 100 ml beaker and 50 ml of ultrapure water was added. This sample was sonicated for 30 minutes in an ultrasonicator. Then, the sample suspension was injected into electrode cell for measurement of zeta potential using zeta analyzer.

Fourier transform infrared spectroscopy (ftir)

The FTIR spectra of nanoclay particles were recorded using a Bruker (TENSOR 27) equipped with an MCT detector. 256 scans were recorded with a resolution of 4 cm^{-1}. In this study, Infrared (IR) spectroscopy gives information about the nature of surface hydroxyl groups like bronsted acid sites, silanols functional groups and identifying types of chemical bonds in a molecule by producing an infrared absorption spectrum that is like a molecular "fingerprint". The most useful infrared region for nanoclay particles based materials characterization lies between 500 and 4000 cm^{-1} (Liu, 2009) [18]. The term infrared covers the range of electromagnetic spectrum between 0.78 and 1000 µm. In the infrared spectroscopy, the wavelength is usually measured in wavenumbers cm^{-1} (wave number = 1/wavelength in centimetres). The preparation of samples, sample and IR transparent material like potassium bromide (KBr) were mixed in the ratio of 2:1 in a mortar and pestle for 30 minutes. Then the mixture was converted into thin pellets by pressing the prepared mixture with a hydraulic or hand press. The pellet, ideally 0.5 to 1 mm thick was then placed in a transmission holder and scanned. Alternatively, solid samples can be dissolved in a solvent such as methylene chloride, and the solution placed onto a single salt plate. Typically, the pellet technique provides good quality spectra with a wide spectral range and no interfering absorbance bands.

Scanning electron microscope (sem)

The surface morphology of the nanoclay particles was characterized by using Scanning electron microscope (SEM-HITACHI: TM-3030).

X-ray diffraction (xrd)

XRD is a powerful technique for determining the crystal structure. One gram of the powdered sample was characterized using X-Ray Diffractometer (Rigaku Ultima IV Powder XRD) with Cu K line as incident radiation and a filter at a scanning rate of 5° s^{-1}. The powdered sample of 0.5 g was

used for measuring the crystalline nature of atoms in the material. The samples were scanned over a range of 2 θ values from 5 to 90° with a scan step size of 0.02° and speed of 0.080 a scan step time of 1s at room temperature 25ºC (Burton, 2009) [5].

Results and Discussion

In order to achieve the objectives of present investigation as outlined earlier, extraction and characterization of nanoclay particles were carried out. The study area is located in different districts of Andhra Pradesh. The characterization of nanoclay particles were studied by using of UV/VIS, Particle Size Analyzer, Zeta Analyzer, FT-IR, XRD, Scanning Electron Microscope, Transmission Electron Microscope. The experimental results are presented and discussed critically drawing support from published literature in this chapter.

Characterization of nanoclay particles

Particle size analyzer (psa)

The nanoclay particles were analyzed using the Dynamic Light Scattering technique for the measurement of the hydrodynamic diameter of nanoclay particles.

The size of nanoclay particles of black soils of Kambaladinne, Lam farm, Rajamahendravaram, Garikapadu, Maruteru were 9.8 nm (Figure 1a), 47.5 nm (Figure 1b), 29.2 nm (figure 1c), 12.9 nm (Figure 1d) and 32.9 nm (Figure 1e) respectively. The Particle size values of black soils were varied from 9.8 to 47.5 nm with a mean value of 26.46 nm. The highest value of 47.5 nm was noticed in the Lam farm village of Guntur district and the lowest value of 9.8 nm was observed in Kambaladinne village of Kurnool district. The viscosity of the dispersion medium of black soils of Kambaladinne, Lam farm, Rajamahendravaram, Garikapadu, Maruteru were 0.894, 0.893, 0.892, 0.894 and 0.893 mPa.s, respectively. The size of nanoclay particles of red soils of Rekulakunta, Anakapalli, *Vizi*anagaram, Tirupati, Utukur, were 12.2 nm (Figure 1f), 37.3 nm (Figure 1g), 11.0 nm (figure 1h), 20.3 nm (Figure 1i) and 29.8 nm (Figure 1j) respectively. The Particle size values of red soils were varied from 11.0 to 37.3 nm with a mean value of 22.12 nm. The highest value of 37.3 nm was noticed in the Anakapalli village of Vishakhapatnam district and the lowest value of 11.0 nm was observed in *Vizi*anagaram district (Figure 1j). The viscosity of the dispersion medium of red soils of Rekulakunta, Anakapalli, *Vizi*anagaram, Tirupati, Utukur, were 0.895, 0.895, 0.894, 0.893 and 0.893 mPa.s, respectively. The size distribution analyses showed that of all collected soil samples were measured in above indicated nanometers. The comprehensive data and size distribution of nanoclay particles extracted black and red soils was shown in figure 7a and 7b.

Zeta potential

The zeta potential of the nanoclay particles was measured by using Particle and zeta analyzer**.** The data showed that (Table 1) zeta potentials of the nanoclay particles of black soils of Kambaladinne, Lam farm, Rajamahendravaram, Garikapadu, Maruteru were (+) 22.5 mV (Figure 2a), (-) 24.6 mV (Figure 2b), (-) 39.6 mV (Figure 2c), (-) 42.2 mV (Figure 2d) and (-) 43.0 mV (Figure 2e) respectively. The data clearly indicated that the four samples of black soils of nanoclay particles had the negative charge; only one nanoclay sample had the positive charge. Zeta potentials of the nanoclay particles of red soils of Rekulakunta, Anakapalli, *Vizi*anagaram, Tirupati, Utukur, were (-) 42.5 mV (Figure 2f), (-) 40.8 mV (Figure 2g), (-) 43.0 mV (Figure 2h), (-) 52.7 mV (Figure 2i) and (-) 69.0 mV (Figure 2j) respectively. The data clearly indicated that the five samples of red soils of nanoclay particles had the negative charge. Recorded a relatively higher negative zeta potential of (-) 69.0 mV in Utukur village of Kadapa district (Figure 2f) clearly indicates that the particles are highly dispersed.

Table 1: Zeta potential and viscosity of nanoclays extracted from the study areas

S. No.	Location	District	Zeta potential (mV)	Viscosity of the dispersion medium (mPa.s)
Black soils				
1	Kambaladinne	Kurnool	22.5	0.894
2	Lam farm	Guntur	-24.6	0.892
3	R.mahendravaram	East Godavari	-39.6	0.893
4	Garikapadu	Krishna	-42.2	0.894
5	Maruteru	West Godavari	-43.0	0.896
Red soils				
6	Rekulakunta	Anantapur	-42.5	0.894
7	Anakapalli	Vishakhapatnam	-40.8	0.893
8	Vizianagaram	Vizianagaram	-43.0	0.896
9	Tirupati	Chittor	-52.7	0.895
10	Utukur	Kadapa	-69.0	0.892

UV-visible (UV-VIS) spectrophotometer

Clays/Nanoclays contain a variety of molecules with different compositions. We have employed UV-VIS absorbance technique in the present study to identify the different classes of clay particles present in the samples through the characteristic absorbance of the specific element present the respective clay type.

The absorbance below 350 nm attribute to silica bonds (Hugo Fernando *et al.*, 2017) and in the present study broad spectra below 350 nm were observed in all the clay samples indicating the presence of silica bonds.

All clay minerals containing iron (>1%) showed oxo-iron charge transfer in the U.V. region-octahedral iron in the 240-262 nm range and tetrahedral iron) around 215nm. Iron intra configurational structure was evident in muscovite, vermiculite (Transvaal), and nontronite (Samuel *et al.*, 1973) [27]. Absorption spectra were observed at 242 nm (Kaolin mineral, Fig. 3a-3d) in the samples of Garikapadu, Lam farm, Maruteru, *Vizi*anagaram. Absorption spectra were observed at 245 nm (Montmorillonite Mineral, Fig. 3e-3f) in the samples of Anakapalli and Rajamahendravaram. Absorption spectra were observed at 250 nm (Vermiculite mineral, Fig. 3g-3j) in the samples of Kambaladinne, Rekulakunta, Utukur and Tirupati.

Fourier transform infrared spectroscopy (ft-ir)

Infrared spectroscopy can result in a positive identification (qualitative analysis) of every different kind of material. In addition, the size of the peaks in the spectrum is a direct indication of the amount of material present. With modern software algorithms, infrared spectroscopy is an excellent tool for qualitative analysis (Kodama *et al.*, 1962) [14].

The Kambaladinne sample showed different characteristic excitation peaks particularly corresponding to 3612- non bound OH group; 2929- alkane (sp^3) C-H stretc.h; 2857- methylene C-H stretc.h; 2358- alkanyl C≡N stretc.h; 1745- Ester C-O stretc.h; 1696-C-N stretc.h; 1650- C = C (aromatic) stretc.h; 1522- carboxylic acid group; 1464- methyl C-H bend; 1031- primary amine C-N stretc.h; 789- CH_3 rocking and Si-C stretc.hing in Si-CH_3; 691- aromatic C-H bend; (Fig. 4a).

The Rekulakunta sample showed different characteristic excitation peaks particularly 3611- non bound OH group; 2929- alkane (sp^3) C-H stretc.h; 2876- methylene C-H stretc.h; 2583- thiol S-H stretc.h; 2351- alkanyl C≡N stretc.h; 1745- Ester C-O stretc.h; 1694- C-N stretc.h; 1519- carboxylic acid; 1000- alkoxy C-O stretc.h; 790- CH3 rocking and Si-C stretc.hing in Si-CH_3; 696- aromatic C-H bend; (Fig. 4b).

The Anakapalli sample showed different characteristic excitation peaks particularly 3613- non bound OH group; 3357- H bonded OH stretc.h; 2931- alkane (sp^3) C-H stretc.h; 2706- CH_2 asymmetric stretc.hing; 2355- alkanyl C≡N stretc.h; 1742- Ester C-O stretc.h; 1691- C-N stretc.h; 1642- 1^0 amine N-H bend; 1521- carboxylic acid; 1398- sp^3 C-H bend; 993- skeletal vibrations; 787- skeletal vibrations; 688- aryl thioether (C-S) stretc.h ; (Fig. 4c).

The Lam farm sample showed different characteristic excitation peaks particularly 3673- alcohol OH stretc.h; 3610- non bound OH group; 3222- SP C-H stretc.h; 2939- alkane (sp^3) C-H stretc.h; 2357- alkanyl C≡N stretc.h; 1745- Ester C-O stretc.h; 1697- C-N stretc.h; 1649- C = C (aromatic) stretc.h; 1523- carboxylic acid group; 1004- alkoxy C-O stretc.h; 917- alkene sp^2 C-H bend; 790- CH_3 rocking and Si-C stretc.hing in Si-CH_3; 684- aromatic C-H bend; (Fig. 4d).

The Rajamahendravaram sample showed different characteristic excitation peaks particularly 3614- non bound OH group; 2932- alkane (sp^3) C-H stretc.h; 2358- alkanyl C≡N stretc.h; 1744- Ester C-O stretc.h; 1696- C-N stretc.h; 1525- carboxylic acid group; 1006-alkoxy C-O stretc.h; 790- CH_3 rocking and Si-C stretc.hing in Si-CH3; 696- aromatic C-H bend; (Fig. 4e).

The Garikapadu sample showed different characteristic excitation peaks particularly 3671- alcohol OH stretc.h; 3611- non bound OH group; 3295- sp C-H stretc.h; 3115- 1^o N-H_2 stretc.h; 2929- alkane (sp^3) C-H stretc.h; 2857- methylene C-H stretc.h; 2588- thiol S-H stretc.h; 2359- alkanyl C≡N stretc.h; 1745- Ester C-O stretc.h; 1696- C-N stretc.h; 1649- C-N stretc.h; 1521- carboxylic acid group; 1464- methyl C-H bend; 1009- alkoxy C-O stretc.h; 791- CH_3 rocking and Si-C stretc.hing in Si-CH_3; 693- aromatic C-H bend; (Fig. 4f).

The *Vizianagaram* sample showed different characteristic excitation peaks particularly 3616- non bound OH group; 2930- alkane (sp^3) C-H stretc.h; 2356- alkanyl C≡N stretc.h; 1694- C-N stretc.h; 1523- carboxylic acid OH stretc.h; 1022-; 787- CH_3 rocking and Si-C stretc.hing in Si-CH_3; 689- aromatic C-H bend; (Fig. 4g).

The Tirupati sample showed different characteristic excitation peaks particularly 3612- non bound OH group; 2929- alkane (sp^3) C-H stretc.h; 2857- methylene C-H stretc.h; 2358- alkanyl C≡N stretc.h; 1745- Ester C-O stretc.h; 1696- C-N stretc.h; 1650- C = C (aromatic) stretc.h; 1522- carboxylic acid group; 1464- methyl C-H bend; 1031- primary amine C-N stretc.h; 789- CH_3 rocking and Si-C stretc.hing in Si-CH_3; 691- aromatic C-H bend; (Fig. 4h).

The Utukur sample showed different characteristic excitation peaks particularly 3673- alcohol OH stretc.h; 3612- non bound OH group; 3230- SP C-H stretc.h; 2930- alkane (sp^3) C-H stretc.h; 2858- thiol S-H stretc.h; 2359- alkanyl C≡N stretc.h; 1745- Ester C-O stretc.h; 1695- C-N stretc.h; 1649- C = C (aromatic) stretc.h; 1520- carboxylic acid group; 1464- methyl C-H bend; 1001- alkoxy C-O stretc.h; 791- CH_3 rocking and Si-C stretc.hing in Si-CH_3; 694- aromatic C-H bend; (Fig. 4i).

The Maruteru sample showed different characteristic excitation peaks particularly 3673- Alcohal OH stretc.h; 3612- non bound OH group; 3230- SP C-H stretc.h; 2930- alkane (sp^3) C-H stretc.h; 2858- methylene C-H stretc.h; 2359- alkanyl C≡N stretc.h; 1917- acid chloride C = O stretc.h; 1745- Ester C-O stretc.h; 1695- C-N stretc.h; 1649- C = C (aromatic) stretc.h; 1520- carboxylic acid group; 1464- methyl C-H bend; 1001- alkoxy C-O stretc.h; 791- CH_3 rocking and Si-C stretc.hing in Si-CH_3; 684-; (Fig. 4j).

The intensity of the peak showing near to 1523 cm^{-1} corresponding to Carboxylic acid salts and that peak at 3612 cm^{-1} corresponding to non-bonded OH group/stretc.h are present in all the samples of black and red soils. The peak near 1742 cm^{-1} was seen in all black soils irrespective of the region but it is interesting to note that the samples from Utukur, Tirupati, and Rekulakunta regions pertaining to red soil also showed the corresponding peak.

Further, all the samples (Figure 4a to 4j) are rich in phosphate and silicate ions which correspond to the peaks in the range of 900 cm^{-1} to 1100 cm^{-1}. Also, the peaks near to 684 cm^{-1} and near to 787 cm^{-1} which are seen in all the samples show the presence of thiols/ethers and aromatic C-H bends respectively.

X-ray diffraction (xrd) analysis

X-ray diffraction identification helps in mineral modification by suitable chemical/ or thermal treatment 7, 10 and 14 Å are the most commonly observed layer spacings. Various experimental techniques are available to examine sufficiently well crystallized material but clay minerals are neither pure nor well crystallized and so difficult to analyzed.

Characteristics at 7, 10 and 14 Å spacings are related to well form kaolin, mica and chlorite 10 and 14 Å show respective hydrated forms such as hydrated halloysite and montmorillonoids. They can be recognized either by low temperature dehydration or by organic complex formation.

Particles size and distribution

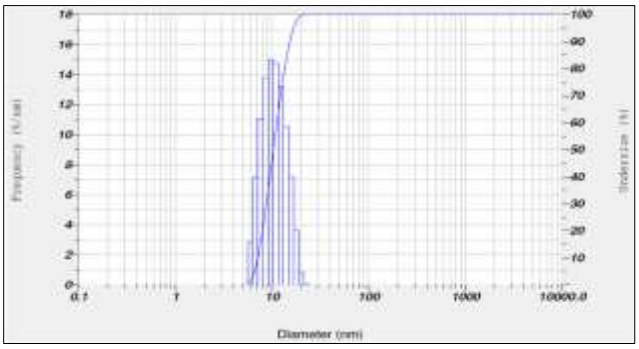

Fig 1a: Histogram of nanoclay particles (mean size 9.8 nm) extracted from Kambaladinne sample (Black soil)

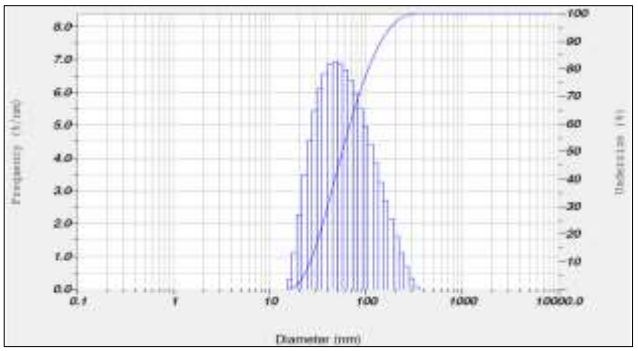

Fig 1b: Histogram of nanoclay particles (mean size 47.5 nm) extracted from Lam farm sample (Black soil)

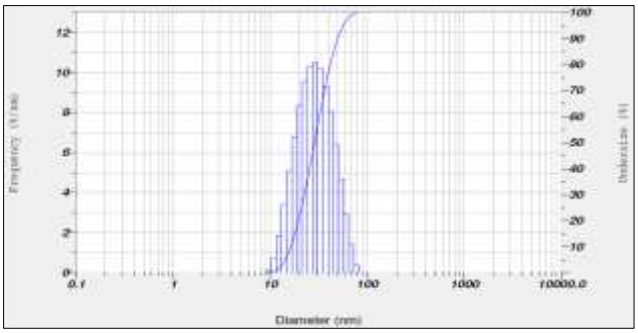

Fig 1c: Histogram of nanoclay particles (mean size 29.2 nm) extracted from Rajamahendravaram sample (Black soil)

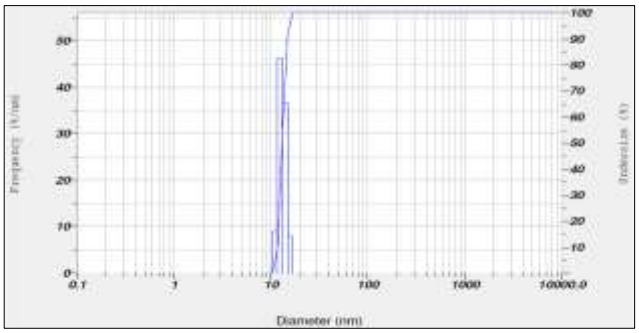

Fig 1d: Histogram of nanoclay particles (mean size 12.9 nm) extracted from Garikapadu sample (Black soil)

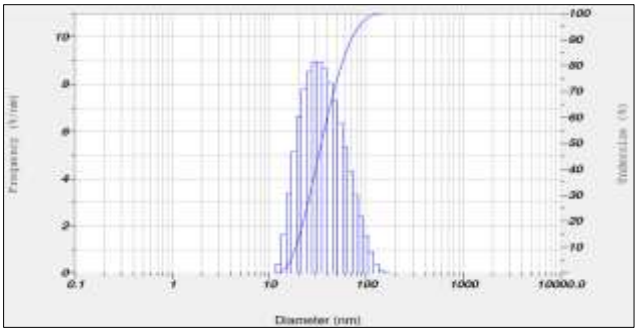

Fig 1e: Histogram of nanoclay particles (mean size 32.9 nm) extracted from Maruteru sample (Black soil)

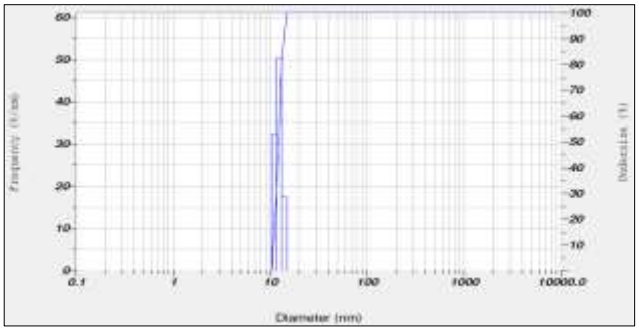

Fig 1f: Histogram nanoscale nanoclay particles (mean size 12.2 nm) extracted from Rekulakunta sample (Red soil)

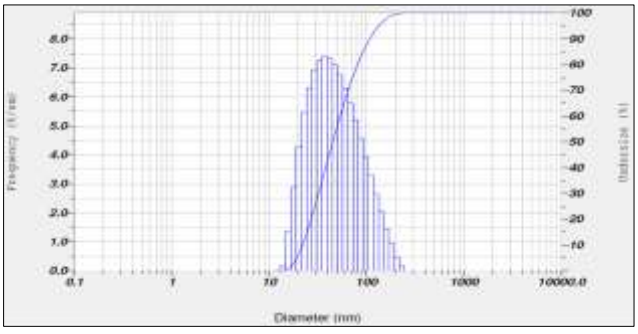

Fig 1g: Histogram of nanoclay particles (mean size 37.3 nm) extracted from Anakapalli sample (Red soil)

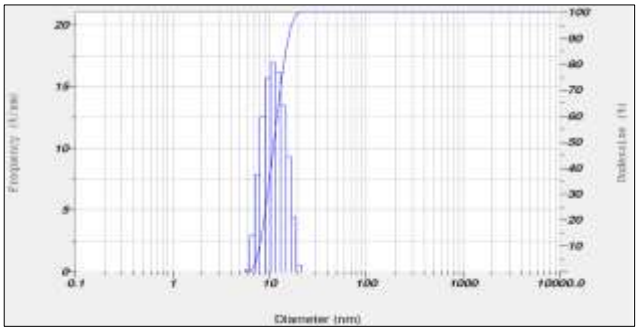

Fig 1h: Histogram of nanoclay particles (mean size 11.0 nm) extracted from *Vizi*anagaram sample (Red soil)

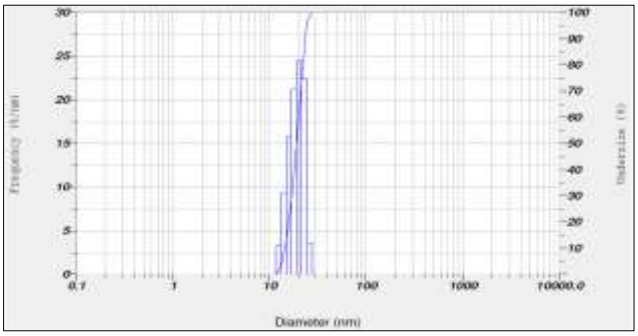

Fig 1i: Histogram of nanoclay particles (mean size 20.3 nm) extracted from Tirupati sample (Red soil)

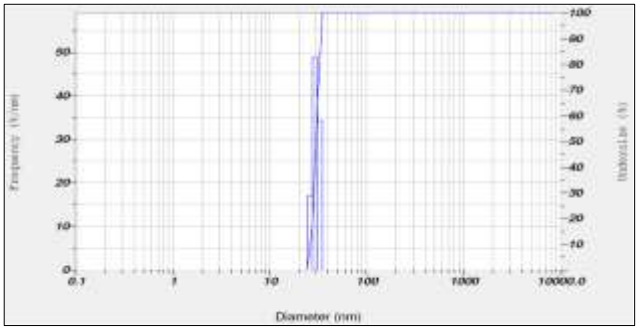

Fig 1j: Histogram of nanoclay particles (mean size 29.8 nm) extracted from Utukur sample (Red soil)

Zeta Potential

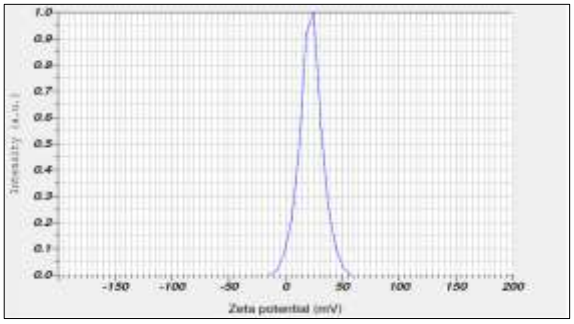

Fig 2a: Zeta potential (+ 22.5 mV) of nanoclay particles extracted from Kambaladinne sample (Black soil)

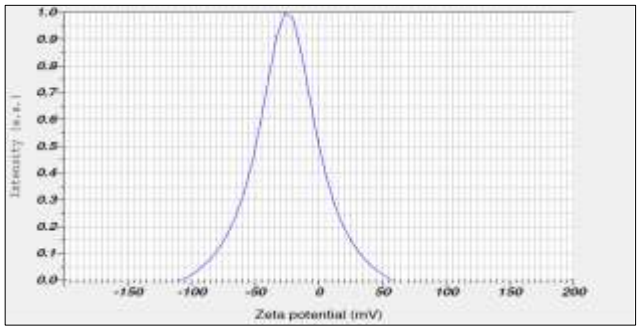

Fig 2b: Zeta potential (-24.6 mV) of nanoclay particles extracted from Lam farm sample (Black soil)

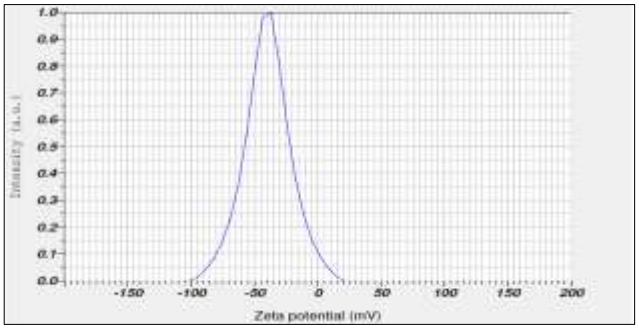

Fig 2c: Zeta potential (-39.6 mV) of nanoclay particles extracted from Rajamahendravaram sample (Black soil)

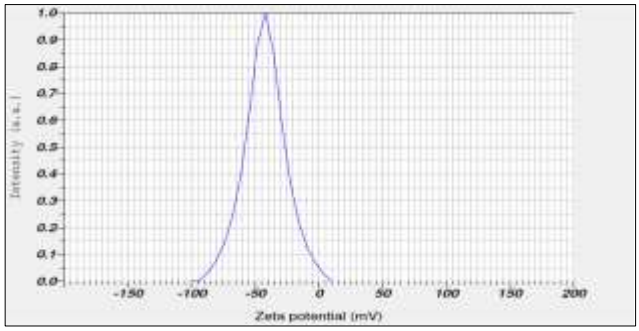

Fig 2d: Zeta potential (-42.2 mV) of nanoclay particles extracted from Garikapadu sample (Black soil)

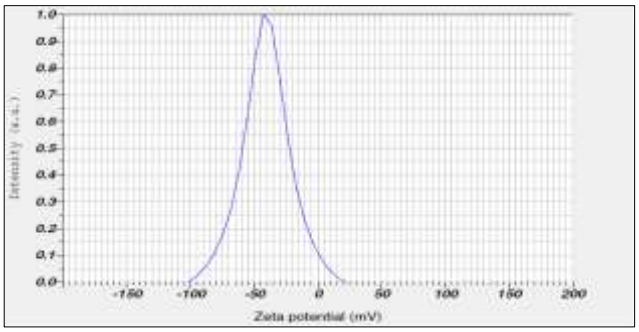

Fig 2e: Zeta potential (-40.6 mV) of nanoclay particles extracted from Maruteru sample (Black soil)

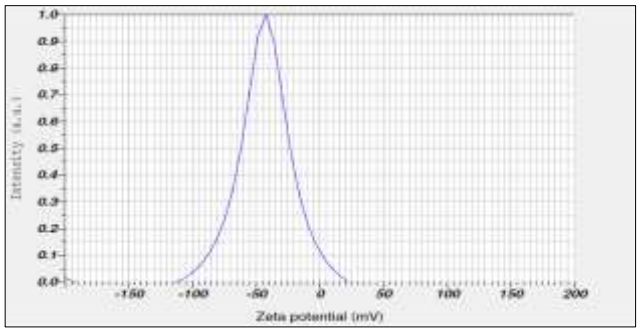

Fig 2f: Zeta potential (-42.5 mV) of nanoclay particles extracted from Rekulakunta sample (Red soil)

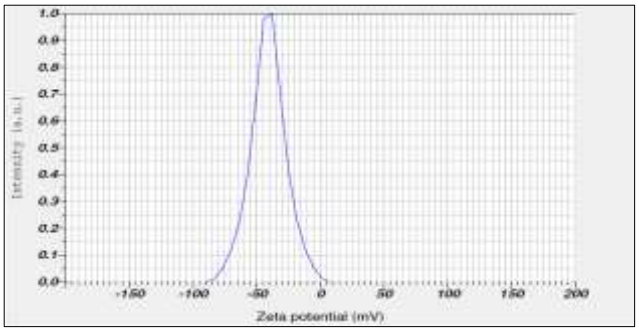

Fig 2g: Zeta potential (-40.8 mV) of nanoclay particles extracted from Anakapalli sample (Red soil)

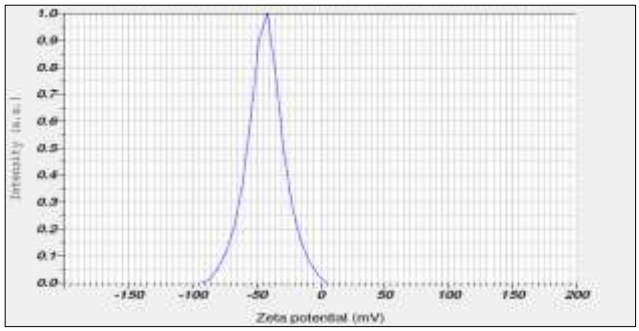

Fig 2h: Zeta potential (-43.0 mV) of nanoclay particles extracted from *Vizi*anagaram sample (Red soil)

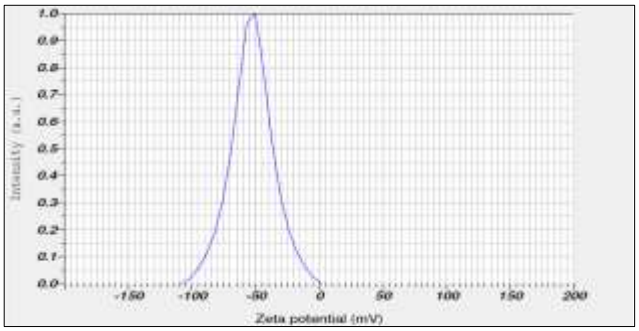

Fig 2i: Zeta potential (-52.7 mV) of nanoclay particles extracted from Tirupati sample (Red soil)

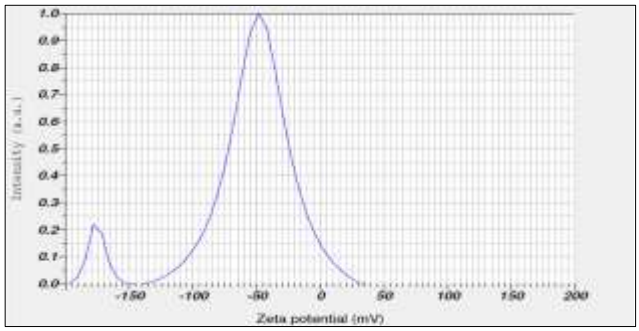

Fig 2j: Zeta potential (-69.0 mV) of nanoclay particles extracted from Utukur sample (Red soil)

UV-visible (UV-VIS) spectrophotometer

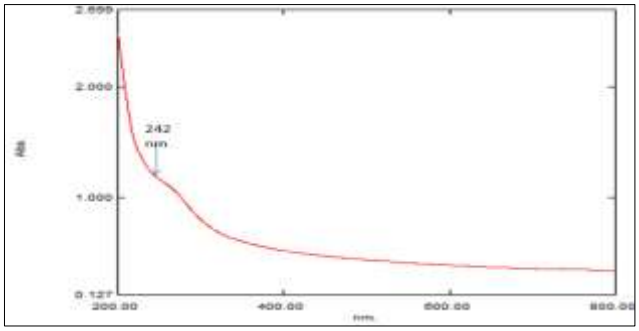

Fig 3a: UV-VIS absorption peak of nanoclay particles at 242 nm extracted from Garikapadu sample

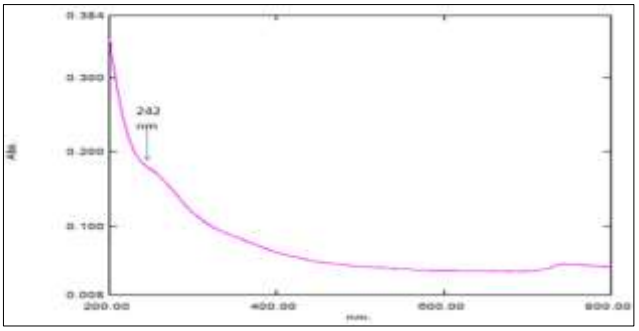

Fig 3b: UV-VIS absorption peak of nanoclay particles at 242 nm extracted from Lam farm sample

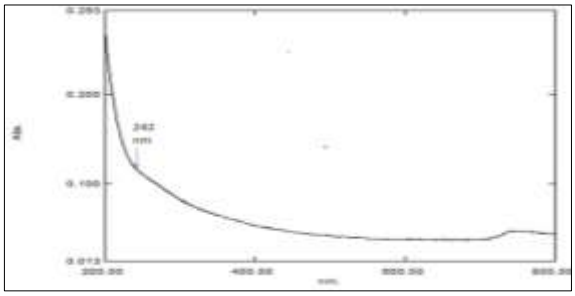

Fig 3c: UV-VIS absorption peak of nanoclay particles at 242 nm extracted from Maruteru sample

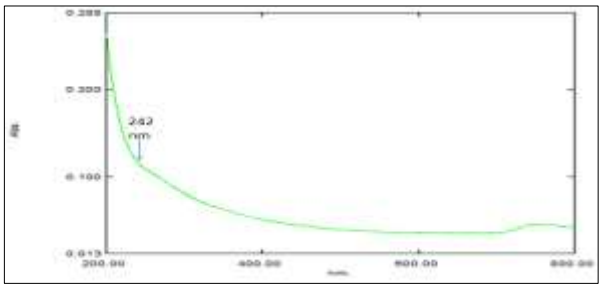

Fig 3d: UV-VIS absorption peak of nanoclay particles at 242 nm extracted from *Vizi*anagaram sample

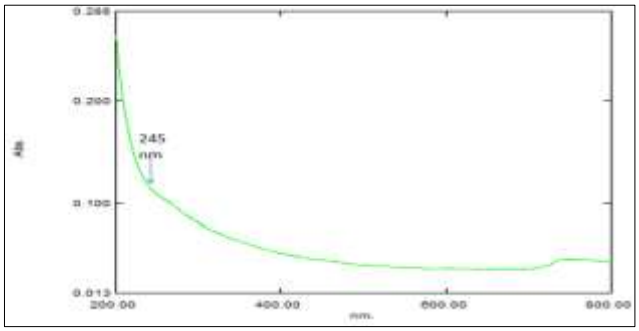

Fig 3e: UV-VIS absorption peak of nanoclay particles at 245 nm extracted from Anakapalli sample

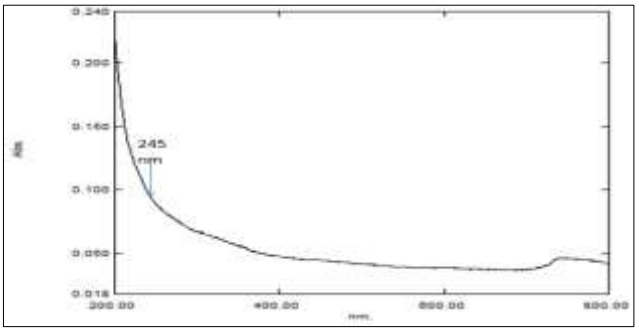

Fig 3f: UV-VIS absorption peak of nanoclay particles at 245 nm extracted from Rajamahendravaram sample

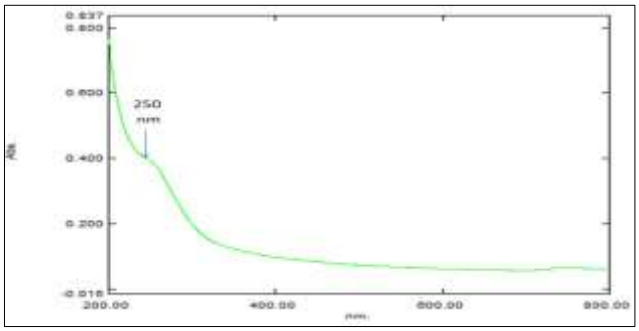

Fig 3g: UV-VIS absorption peak of nanoclay particles at 252 nm extracted from Kambaladinne sample

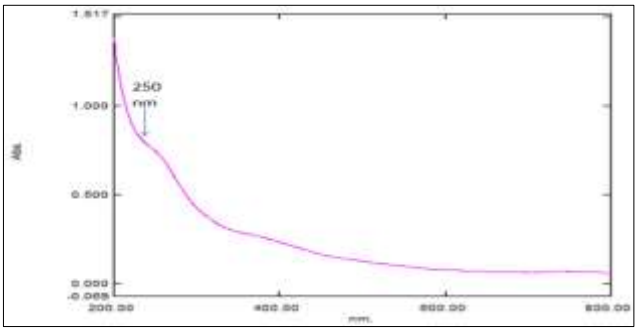

Fig 3h: UV-VIS absorption peak of nanoclay particles at 250 nm extracted from Rekulakunta sample

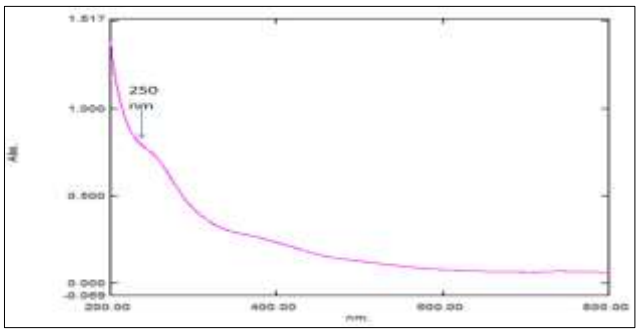

Fig 3i: UV-VIS absorption peak of nanoclay particles at 250 nm extracted from Kadapa sample

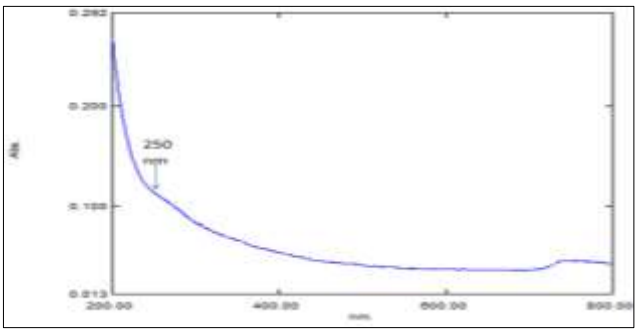

Fig 3j: UV-VIS absorption peak of nanoclay particles at 250 nm extracted from Tirupati sample

Fourier Transform Infrared Spectroscopy (FT-IR)

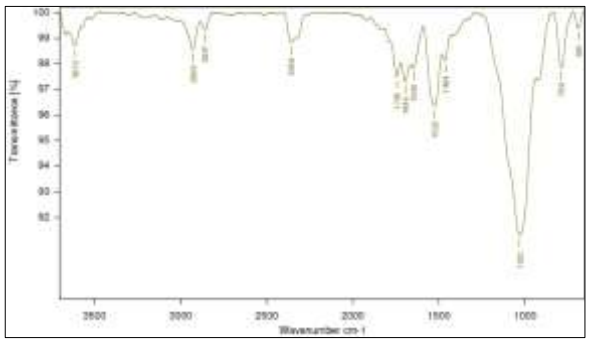

Fig 4a: FT-IR micrograph confirming the presence of different functional groups on the surface of the nanoclay particles extracted from Kambaladinne sample (Black soil)

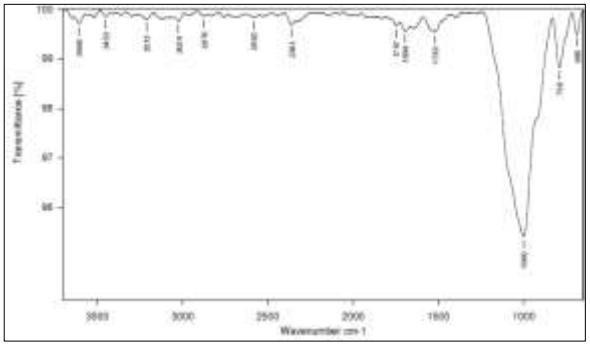

Fig 4b: FT-IR micrograph confirming the presence of different functional groups on the surface of the nanoclay particles extracted from Rekulakunta sample (Red soil)

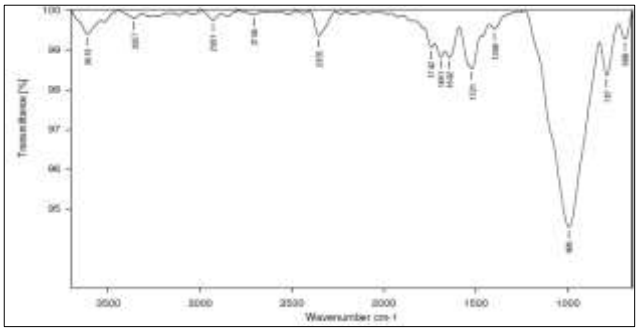

Fig 4c: FT-IR micrograph confirming the presence of different functional groups on the surface of the nanoclay particles extracted from Anakapalli sample (Red soil)

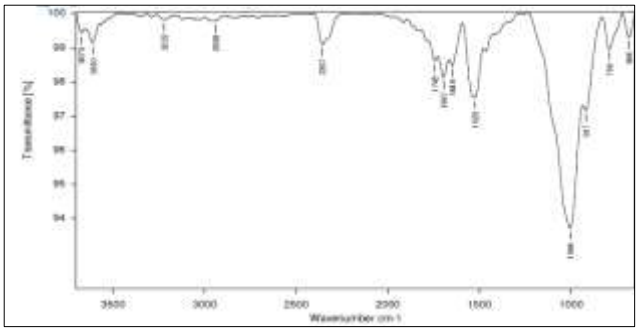

Fig 4d: FT-IR micrograph confirming the presence of different functional groups on the surface of the nanoclay particles extracted from Lam farm sample (Black soil)

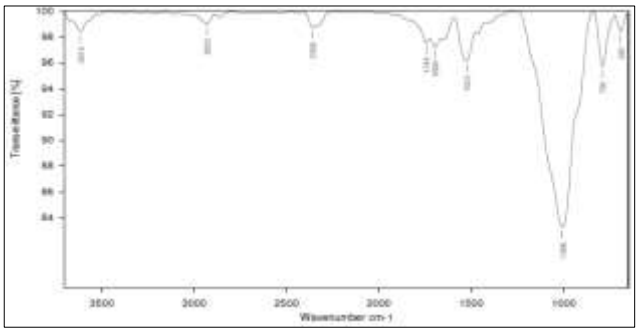

Fig 4e: FT-IR micrograph confirming the presence of different functional groups on the surface of the nanoclay particles extracted from Rajamahendravaram sample (Black soil)

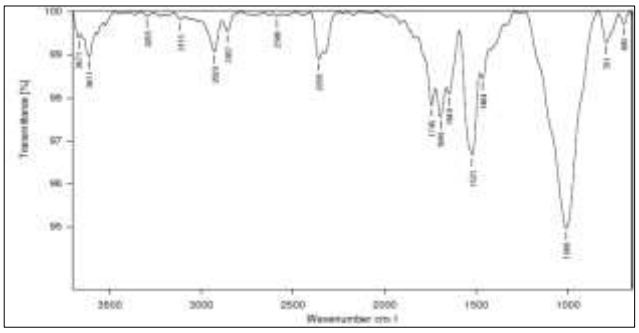

Fig 4f: FT-IR micrograph confirming the presence of different functional groups on the surface of the nanoclay particles extracted from Garikapadu sample (Black soil)

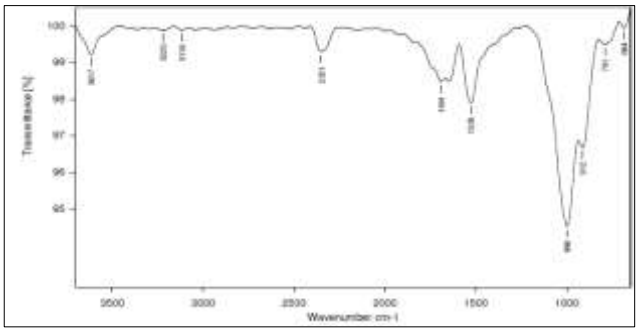

Fig 4g: FT-IR micrograph confirming the presence of different functional groups on the surface of the nanoclay particles extracted from *Vizi*anagaram (Red soil)

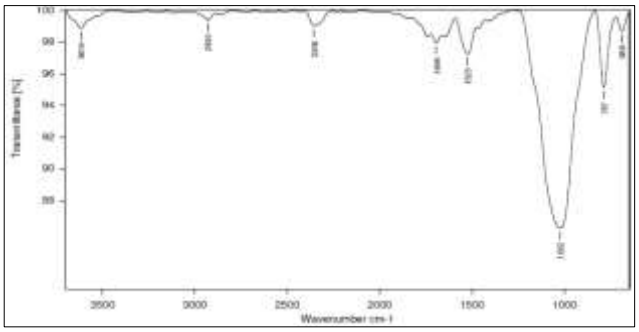

Fig 4h: FT-IR micrograph confirming the presence of different functional groups on the surface of the nanoclay particles extracted from Tirupati sample (Red soil)

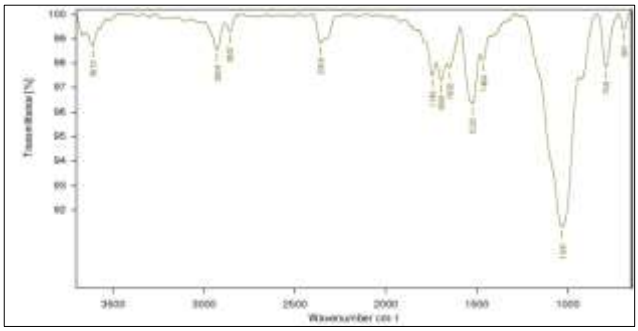

Fig 4i: FT-IR micrograph confirming the presence of different functional groups on the surface of the nanoclay particles extracted from Utukur sample (Red soil)

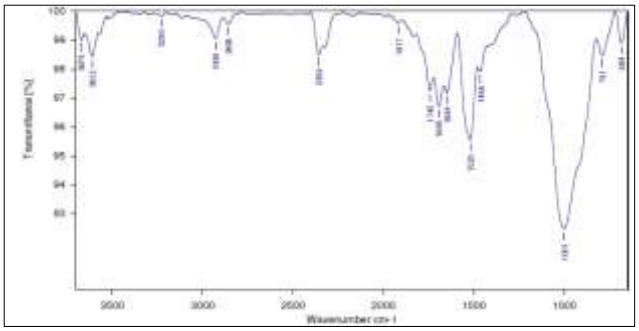

Fig 4j: FT-IR micrograph confirming the presence of different functional groups on the surface of the nanoclay particles extracted from Maruteru sample (Black soil)

X-ray diffraction (XRD) analysis

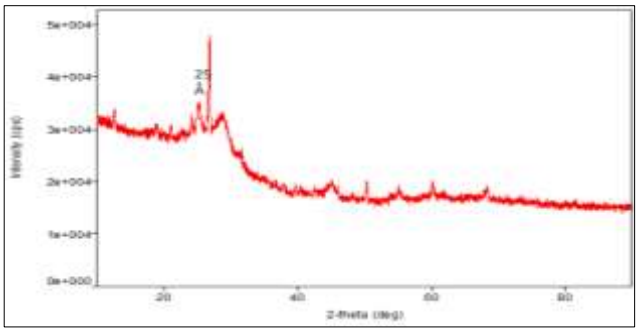

Fig 5a: Random oriented powder XRD pattern of Rectorite, Pyrophyllite type and vermiculite type layers in nanoclay particle extracted from Kambaladinne sample (Black soil)

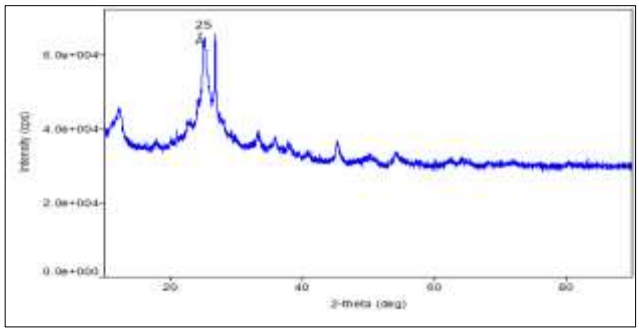

Fig 5b: Random oriented powder XRD pattern of Rectorite, Pyrophyllite type and vermiculite type layers in nanoclay particle extracted from Rekulakunta sample (Red soil)

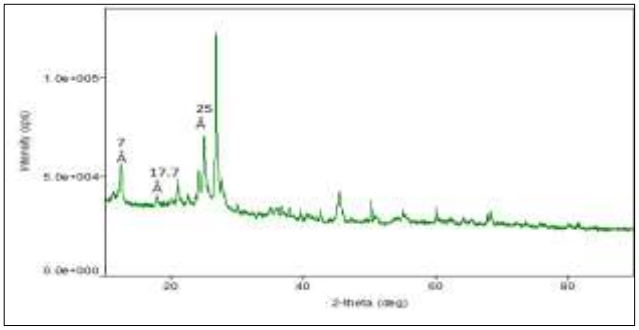

Fig 5c: Random oriented powder XRD pattern of Kaolin, Montmorillonite Rectorite, Pyrophyllite type and vermiculite type layers in nanoclay particle extracted from Anakapalli sample (Red soil)

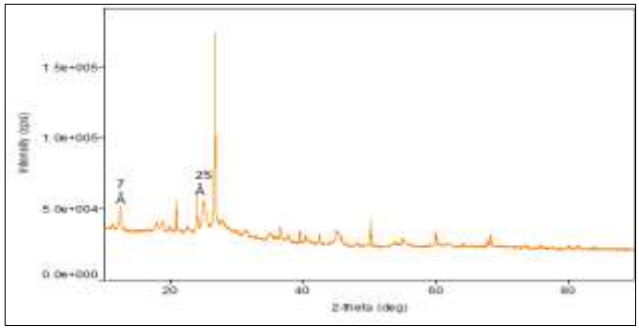

Fig 5d: Random oriented powder XRD pattern of Kaolin, Rectorite, Pyrophyllite type and vermiculite type layers Nanoclay particle extracted from Lam farm sample (Black soil)

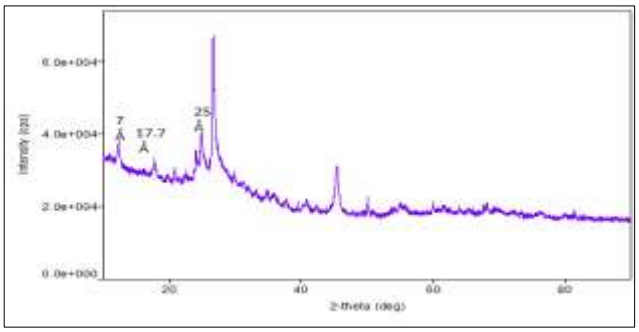

Fig. 5e: Random oriented powder XRD pattern of Kaolin, Montmorillonite, Rectorite, Pyrophyllite type and vermiculite type layers in nanoclay particle extracted from Rajamahendravaram sample (Black soil)

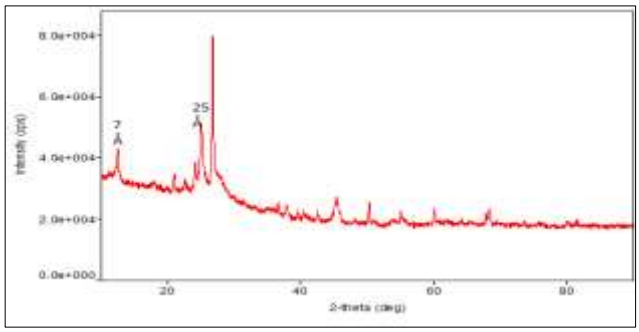

Fig 5f: Random oriented powder XRD pattern of Kaolin, Rectorite, Pyrophyllite type and vermiculite type layers in Nanoclay particle extracted from Garikapadu sample (Black soil)

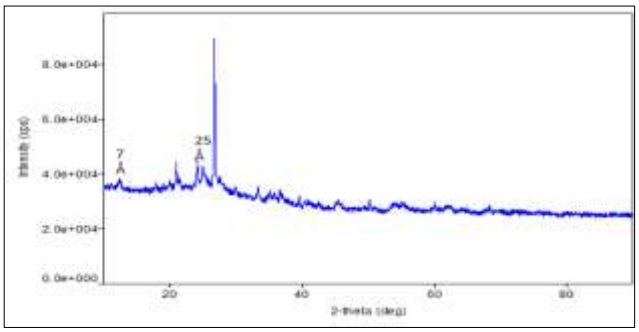

Fig 5g: Random oriented powder XRD pattern of Kaolin, Rectorite, Pyrophyllite type and vermiculite type layers in nanoclay particle extracted from *Vizi*anagaram sample (Red soil)

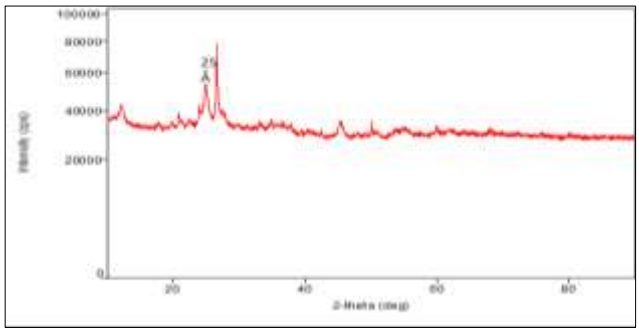

Fig 5h: Random oriented powder XRD pattern of Rectorite, Pyrophyllite type and vermiculite type layers in nanoclay particle extracted from Tirupati sample (Red soil)

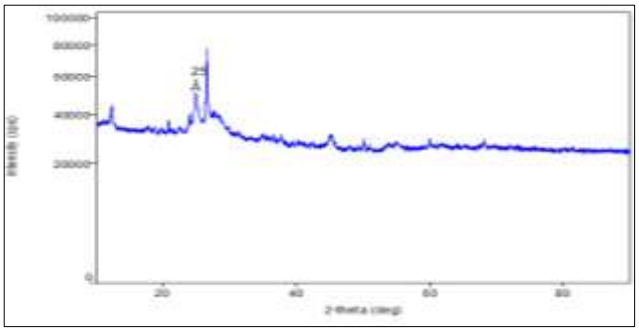

Fig 5i: Random oriented powder XRD pattern of Rectorite, Pyrophyllite type and vermiculite type layers in nanoclay particle extracted from Utukur sample (Red soil)

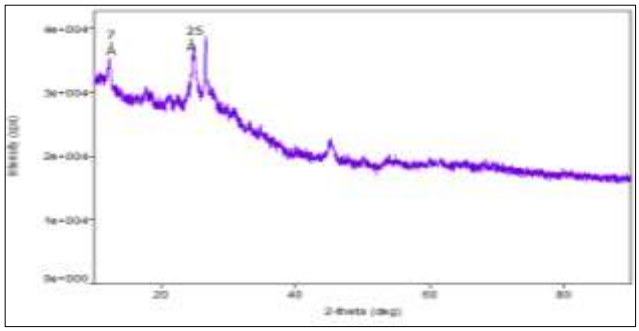

Fig 5j: Random oriented powder XRD pattern of Kaolin, Rectorite, Pyrophyllite type and vermiculite type layers in Nanoclay particle extracted from Maruteru sample (Black soil)

Scanning electron microscopy (SEM)

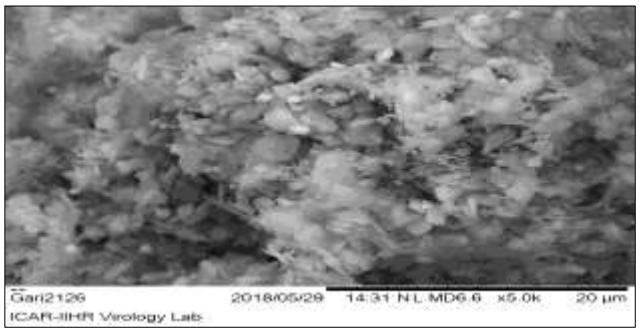

Fig 6a: Curved matted spiny and flocculated flakes in the nanoclay samples of black soils of Garikapadu (Scale bar 20µm)

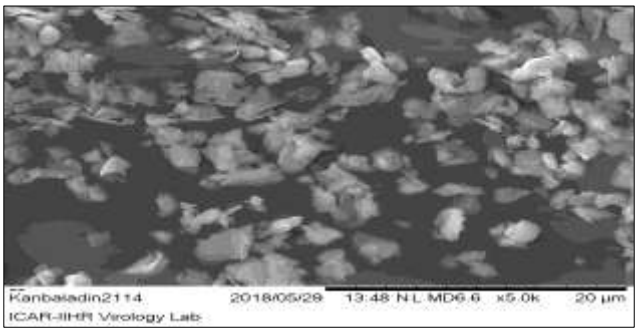

Fig 6b: Curved and matted flakes in the nanoclay samples of black soils of Kambaladinne (Scale bar 20µm)

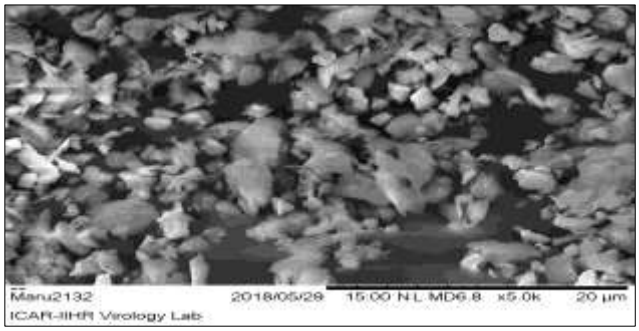

Fig 6c: Curved and matted flakes in the nanoclay samples of black soils of Maruteru (Scale bar 20µm)

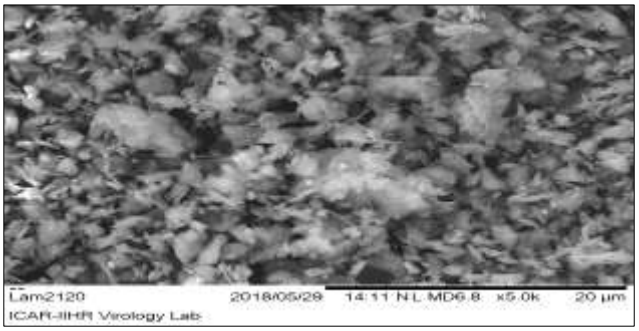

Fig 6d: Spiny and flocculating flakes in the nanoclay samples of black soils of Lam farm (Scale bar 20µm)

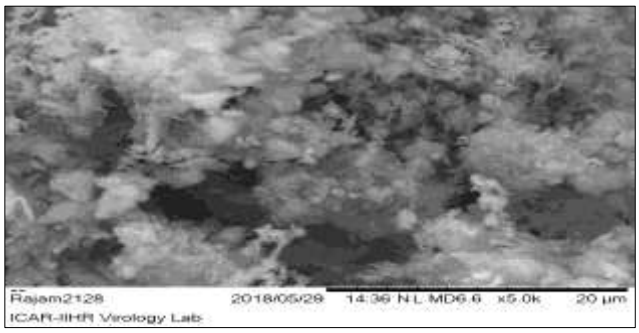

Fig 6e: Spiny and flocculating flakes in the nanoclay samples of black soils of Rajamahendravaram (Scale bar 20µm)

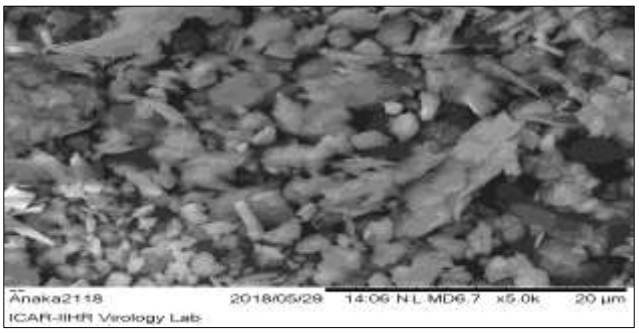

Fig 6f: Curved and matted flakes in the nanoclay samples of red soils of Anakapalli (Scale bar 20µm)

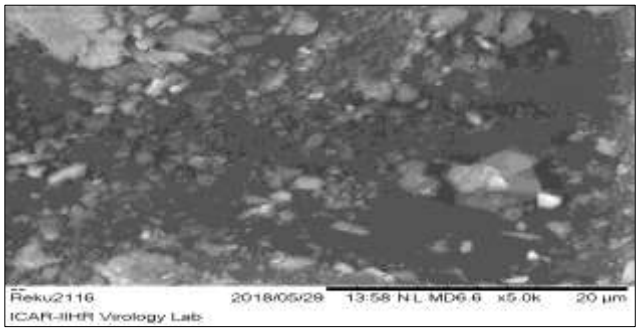

Fig 6g: Spiny and flocculating flakes in the nanoclay samples of red soils of Rekulakunta (Scale bar 20µm)

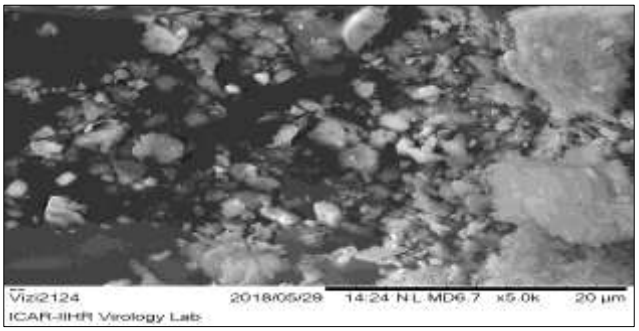

Fig 6h: Spiny and flocculating flakes in the nanoclay samples of red soils of *Viz*ianagaram (Scale bar 20µm)

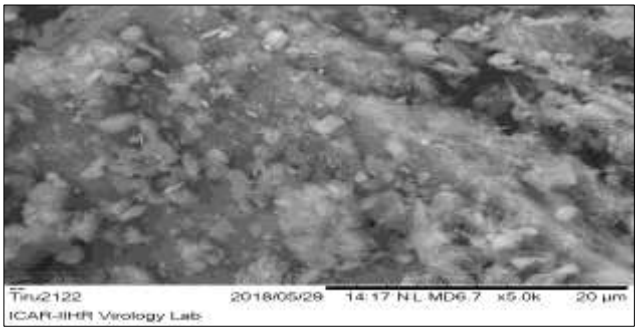

Fig 6i: Spiny and flocculating flakes in the nanoclay samples of red soils of Tirupati (Scale bar 20µm)

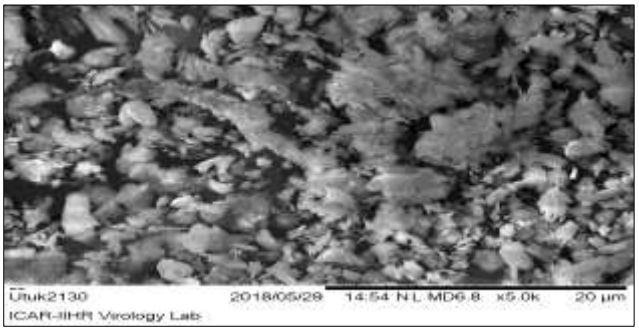

Fig 6j: Spiny and flocculating flakes in the nanoclay samples of red soils of Utukur (Scale bar 20µm)

Variation in the sizes of nanoclay particles extracted from the black and red soils

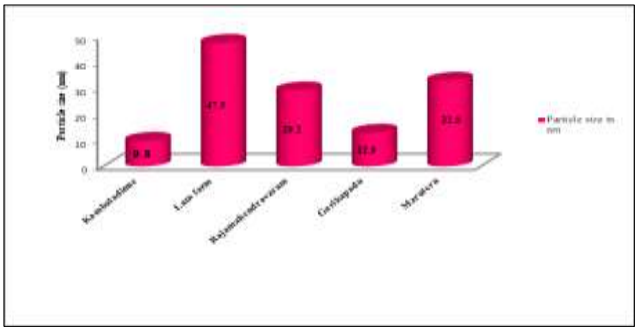

Fig 7a: Variation of particle sizes (nm) of nanoclay particle extracted from blacksoils of Andhra Pradesh

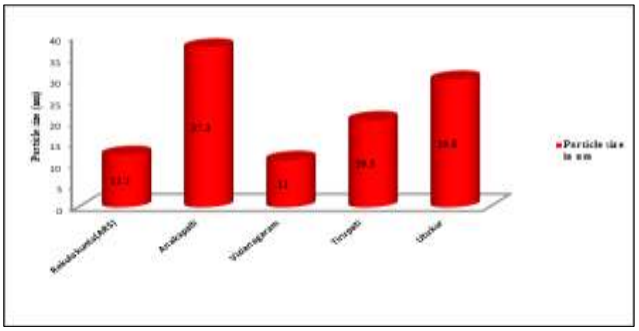

Fig 7b: Variation of particle sizes (nm) of nanoclay particle extracted from red soils of Andhra Pradesh

7 Å indicates a kaolin type mineral (Brindley, 1961) [4] which includes minerals with same kind of layer structure namely kaolin minerals proper, serpentine minerals, chamosite, amesite etc. The presence of Kaoline in the clay samples of Anakapalli, Lam farm, Rajamahendravaram, Garikapadu, *Viz*ianagaram and Maruteru was observed. 25 Å is characteristic of mineral rectorite which contains a regular alternation of Pyrophyllite type and vermiculite type layers. In the present study, the collected clay sample of all black soils and red soils were showed presence of rectorite with characteristics 25 Å spacing. 17.7 Å reflection shows presence of Montmorilonites (Macewan, 1946) [19]. In present context samples of Anakapalli and Rajamahendravaram shows 17.7 Å spacing while remaining were not significant any specific reflections clay material.

Scanning electron microscopy (SEM)

SEM examination revealed a natural clay morphology of very fine, irregular, curved flakes and mats of coalesced flakes. The flakes seem to be anhedral, but it was difficult to determine their exact texture because of particle coalescence (Tatjana Novakovic *et al.*, 2008) [22]. In the present study, curved and matted flakes were observed in the nanoclay samples of black soils of Garikapadu, Kambaladinne and Maruteru while the nanoclay samples of black soils of Lam farm, Rajamahendravaram, Garikapadu have shown a combination of spiny and flocculating flakes. The nanoclay samples of red soils of Anakapalle have shown curved and matted flakes while the nanoclay samples of red soils of Rekulakunta, *Viz*ianagaram, Tirupati and Utukur have shown a combination of spiny and flocculating flakes.

Conclusion

DLS analyzer revealed that there were significant differences were noticed in the size of the particles (range from 9.8 nm to 47.8 nm) with non-significant variations in viscosity (range from 0.892-0.895mPa.s) of both types. However, it was observed a wide range of difference in the zeta potential.

Nanoclay particles from black soil were proven to be less stable with a least zeta potential of + 22.5 mV (Kambaladinne) and red soil of high stability and dispersion with a highest zeta potential of -69 mV (Utukur). It was surprising to note that both of the samples belong to black and red soils.

It is evident from the UV-VIS spectra that corresponding to the presence of silica from 242 to 250 nm was seen in all samples. The peak corresponding at 242 nm revealed the presence of Kaolin mineral in the samples of Garikapadu, Lam faram, Maruteru, *Viz*ianagaram, while the peak corresponding at 245 nm corresponds to the presence of Montmorillonite mineral in the samples of Anakapalli and Rajamahendravaram. The peak corresponding at 250 nm revealed the presence of Vermiculite mineral in the samples of Kambaladinne, Rekulakunta, Utukur, and Tirupati.

Further, the FTIR data revealed that carboxylic acid salts (1523 cm^{-1}), phosphate (900 cm^{-1}) and silicon ions (1100 cm^{-1}), thiols/ethers (684 cm^{-1}) in all the samples irrespective of black and red soils and alkyl carbonates (1742 cm^{-1}) were seen in all black soil samples and also exclusively in the red soil samples of Rayalaseema region.

The crystal structure analyses revealed that Kaolin was present exclusively in the clay samples of collected from Maruteru, Garikapadu, Rajamahendravaram (7 Å spacing) and Rectorite characteristic to 25.0 Å spacing was seen in both types of soil but Montmorilonites (17.7 Å) was detected only in the samples of Anakapalli and Rajamahendravaram.

Electron microscopy showed curved and matted flakes black soil samples collected from Garikapadu, Kambaladinne and Maruteru. The sample collected from Lam farm, Rajamahendravaram, Garikapadu have shown a combination of spiny and flocculating flakes. Red soils of Anakapalli have shown curved and matted flakes while that of Rekulakunta, *Viz*ianagaram, Tirupati and Utukur samples have shown a combination of spiny and flocculating flakes.

Therefore, herein, we have successfully extracted a well-defined nanoclay particles from vertisols (black soils) and alfisols (red soils) through a novel approach and as prepared nanoclay particles could be used as hosts for a number of inorganic and organic compounds which could have numerous applications in agriculture and environmental remediation processes.

Summary

Methods need to be developed to enhance the yield of nanoclay from clay particles. Further studies on the extracted nanoclay particles to examine their thermal stability, surface chemistry and surface area to find suitable avenues for application of extracted nanoclay particles based composites/materials.

References

1. Abidin Z, Matsue N, Henmi T. Differential formation of allophane and imogolite: experimental and molecular orbital study. Journal of Computer-Aided Materials Design 2007;14:5-18.
2. Aitken RJ, Chaudhry MQ, Boxall ABA, Hull M. Manufacture and use of nanomaterials: current status in the UK and global trends. Occupational Medicine-Oxford 2006;56:300–306.
3. Asadi A, Huat BBK, Hanafi MM, Mohamed TA, Shariatmadari N. Role of organic matter on electro-osmotic properties and Ionic modification of organic soils. Geosciences Journal 2009;13(2):175-181.
4. Brindley GW. Kaolin, serpentine, and kindred minerals, and chlorite minerals in the X. ray identification and crystal structures of clay minerals, 2nd Edition. Mineralogical Society. London 1961, P260-266.
5. Burton. Powder Diffraction in Zeolite Science. In Zeolite Characterization and Catalysis. Springer Science Business Media 2009, P1-65.
6. Cebron A, Beguiristain T, Devisme JB, Denonfoux J, Faure P, Lorgeoux C *et al*. Impact of clay mineral, wood sawdust or root organic matter on the bacterial and fungal community structures in two aged PAH-contaminated soils. Environmental Science and Pollution Research 2015;22(18):13724-13738.
7. Diallo MS, Savage N. Nanoparticles and water quality. Journal of Nanoparticle Research 2005;7:325-330.
8. Floody MC, Theng BKG, Reyes P, Mora ML. Natural nanoclays: applications and future trends – a Chilean perspective. Clay Minerology 2009;44:161-176.
9. Garrido-Ramirez EG, Theng BKG, Mora ML. Clays and oxide minerals as catalysts and nanocatalysts in Fenton-like reactions – A review. Applied Clay Science 2010;47:182-192.
10. Hochella MF, Lower SK, Maurice PA, Penn RL, Sahai N, Sparks DL *et al*. Nanominerals, mineral nanoparticles, and Earth systems. Science 2008;319:1631-1635.
11. Hofmann S, Sharma R, Wirth CT, Cervantes-Sodi F, Ducati C, Kasama T *et al*. Ledge-flow-controlled catalyst interface dynamics during Silicon nanowire growth. Nature materials 2008;7:372-375.
12. Jackson ML. Soil chemical analysis. Prentice Hall of India Pvt. Ltd., New Delhi, India 1973, P1-498.
13. Jeon HS, Rameshwaram JK, Kim G, Weinkauf DH. Characterization of polyisoprene - clay nanocomposites prepared by solution blending. Polymer 2003;44:5749-5758.
14. Kodama H, Oinuma K. Identification of kaolin minerals in the presence of chlorite by x-ray diffraction and infrared absorption spectra.Clay and Clay Minerals 1962;11(1):236-249.
15. Kuzniatsova T, Kim Y, Shqau K, Dutta PK, Verweij H. Zeta potential measurements of zeolite Y: Application in homogeneous deposition of particle coatings. Microporous Mesoporous Materials 2007;103(1-3):102-107.
16. Lepoittevin B, Devalckenaere M, Pantoustier N, Alexandre M, Kubies D, Calberg C *et al*. Poly (ε-caprolactone)/clay nanocomposites prepared by melt intercalation: mechanical, thermal and rheological properties. Polymer 2002;43:4017-4023.
17. Li Z, Hu N. Direct electrochemistry of heme proteins in their layer-by-layer films with clay nanoparticles. Journal of Electroanalytical Chemistry 2003;16:558-155.
18. Liu. Infrared and Raman Spectroscopy in Zeolite Characterization and Catalysis. Springer Science Business Media 2009, 197-222.
19. Macewan DMC. The identification and estimation of montmorillonite group of minerals, with special reference to soil clays: Society of Chemical Industry Journal 1946;65:298-304.
20. Majeed K, Jawaid M, Hassan A, Abu Bakar A, Abdul Khalil HPS *et al*. Potential materials for food packaging from nanoclay/natural fibers filled hybrid composites. Materials and Design 2013;46:391-410.

21. Murr LE, Esquivel EV, Bang JJ, de la Rosa G, Gardea Torresdey JL. Chemistry and nanoparticulate compositions of a 10, 000 year-old ice core melt water. Water Research 2004;38:4282-4296.
22. Novakovic T, Rozic L, Petrovic S, Rosic A. Synthesis and characterization of acid-activated Serbian smectite clays obtained by statistically designed experiments. Chemical Engineering Journal 2008;137(2):436-442.
23. Nowack B, Bucheli TD. Occurrence, behavior and effects of Nanoparticles in the environment. Environmental pollution 2007;150:5-22.
24. Parfitt RL, Russell M, Orbell GE. Weathering sequence of soils from volcanic ash involving allophane and halloysite, Newzealand. Geoderma 1983;29:41-57.
25. Pranzas PK, Willumeit R, Gehrke R, Thieme J, Knochel A 2003.
26. Ryan JN, Elimelech M. Colloid mobilization and transport in groundwater. Elsevier 1996;107:1-56.
27. Samuel Karickhoff W, George WB. Optical absorption spectra of clay minerals. Clays and Clay minerals 1973;29:59-70.
28. Theng BKG, Yuan G. Nanoparticles in the Soil Environment. Elements 2008;4:395-399.
29. Turpault MP, Righi D, Uterano C. Clay minerals: precise markers of the spatial and temporal variability of the biogeochemical soil environment. Geoderma 2008;147:108-115.
30. Wada K. Minerals formed and mineral formation from volcanic ash by weathering. Chemical Geology 1987;60:17-28.
31. Wada K. Minerals formed and mineral formation from volcanic ash by weathering. Chemical Geology 1987;60:17-28.
32. Waychunas GA, Kim CS, Banfield JF. Nanoparticulate iron oxide minerals in soils and sediments: unique properties and contaminant scavenging mechanisms. Journal of Nanoparticle Research 2005;7:409-433.
33. Wilson MA, Tran NH, Milev AS, Kannangara GSK, Volk H, Lu GQM. Nanomaterials in soils. Geoderma 2008;146:291-302.
34. Zhang D, Zhou CH, Lin CX, Tong DS, Yu WH. Synthesis of clay minerals. Applied Clay Science 2010;50:1-11.